National Cancer Institute, although not against P388 lymphocytic leukemia.

The data in Table IV was generated as follows. Compound IIa was dissolved in saline and administered to mice hosting tumors 1–3 by the subcutaneous route and intraperitoneally in the remaining cases. The xenografts (tumors 1–3) were inoculated into NU/NU athymic Swiss mice by subcutaneous injection. The activity recorded is the mean tumor weight change between day 0 and the final evaluation days which were 15, 11, and 11 d, respectively. The $CD8F_1$ mammary and colon 38 tumors in $CD8F_1$ and $B_6C_3F_1$ mice, respectively, were evaluated after 34 and 20 d. The activity noted for the $CD8F_1$ mammary tumor was the median tumor weight change, and for the colon 38 tumor, the median tumor weight was estimated from the diameter of the tumor. The B16 melanocarcinoma was injected intraperitoneally into $B_6C_3F_1$ mice and evaluated on day 60. Both L1210 and P388 leukemias were injected by the intraperitoneal route into CD_2F_1 mice and evaluated on day 30. The Lewis lung carcinoma was injected intravenously into $B_6C_3F_1$ mice and evaluated on day 60. The activity of the last four tumors is expressed as the effect on median survival time. The toxicity of IIa *versus* the nine tumors listed in Table IV was evaluated on days 15, 11, 11, 34, 20, 5, 5, 5, and 5, respectively.

Disposition Studies with IIa—Dosed male Wistar rats, weighing 220–250 g (first trial), 285–300 g (second trial), and 240–250 g (third trial) were injected with IIa dissolved in sterile saline (0.9% w/v) by the intraperitoneal route, while control animals received sterile saline (0.9% w/v). All animals were necropsied after sacrifice, and the following tissues were fixed in 10% buffered formalin: lung, heart, thymus, trachea, thyroid, liver, spleen, pancreas, kidney, adrenal, stomach, duodenum, jejunum, ileum, cecum, colon, rectum, lymph nodes, bladder, and reproductive organs. Tissues were processed routinely, sectioned at 5 μm, and stained with hematoxylin and eosin.

REFERENCES

(1) J. R. Dimmock, C. B. Nyathi, and P. J. Smith, *J. Pharm. Sci.*, **67**, 1543 (1978).

(2) J. R. Dimmock, G. B. Baker, and R. G. Sutherland, *Can. J. Pharm. Sci.*, **10**, 53 (1975).

(3) J. R. Dimmock and W. G. Taylor, *J. Pharm. Sci.*, **64**, 241 (1975).

(4) F. A. Carey and R. J. Sundberg, "Advanced Organic Chemistry, Part B: Reactions and Synthesis," Plenum, New York, N.Y., 1977, pp. 44, 46.

(5) F. F. Blicke, in "Organic Reactions," Vol. 1, R. Adams, Ed., Wiley, New York, N.Y., 1942, p. 303.

(6) F. W. Menger and J. H. Smith, *J. Am. Chem. Soc.*, **91**, 4211 (1969).

(7) C. E. Lough, D. J. Currie, and H. L. Holmes, *Can. J. Chem.*, **46**, 771 (1968).

(8) P. N. Gordon, J. D. Johnston, and A. R. English in "Antimicrobial Agents and Chemotherapy," G. L. Hobby, Ed., American Society for Microbiology, Ann Arbor, Mich., 1965, p. 165.

(9) H. Schönenberger, T. Bastug, L. Bindl, A. Adam, D. Adam, A. Petter, and W. Zwez, *Pharm. Acta. Helv.*, **44**, 691 (1969).

(10) J. R. Dimmock, K. Shyam, N. W. Hamon, B. M. Logan, S. K. Raghavan, D. J. Harwood, and P. J. Smith, *J. Pharm. Sci.*, **72**, 887 (1983).

(11) M. Eden, B. Haines, and H. Kahler, *J. Natl. Cancer Inst.*, **16**, 541 (1955).

(12) H. Kahler and W. v B. Robertson, *J. Natl. Cancer Inst.*, **3**, 495 (1943).

(13) K. A. Meyer, E. M. Kammerling, L. Amtman, M. Koller, and S. J. Hoffman, *Cancer Res.*, **8**, 513 (1948).

(14) A. Albert and E. J. Serjeant, "Ionisation Constants of Acids and Bases," Methuen, London, 1962, pp. 140–141.

(15) A. Bongini, G. Cardillo, M. Orena, and S. Sandri, *Synthesis*, **1979**, 618.

(16) F. A. Carey and R. J. Sundberg, "Advanced Organic Chemistry, Part A: Structure and Mechanisms," Plenum, New York, N.Y., 1977, p. 145.

(17) C. E. Maxwell, *Org. Syn.*, **23**, 30 (1943).

(18) A. H. Land, C. Ziegler, and J. M. Sprague, *J. Am. Chem. Soc.*, **69**, 125 (1947).

(19) A. L. Williams and A. R. Day, *J. Am. Chem. Soc.*, **74**, 3875 (1952).

(20) O. R. Hansen and R. Hammer, *Acta. Chim. Scand.*, **7**, 1331 (1953).

(21) A. Goldin, S. A. Schepartz, J. M. Vendetti, and V. T. DeVita, Jr., "Methods in Cancer Research," Vol. XVI Part A, Academic, New York, N.Y., 1979, p. 165.

(22) J. H. Burkhalter, W. D. Dixon, M. L. Black, R. D. Westland, L. M. Werbel, H. A. DeWald, J. D. Rice, G. Rodney, and D. H. Kaump, *J. Med. Chem.*, **10**, 567 (1967).

(23) H. A. Albrecht, J. T. Plati, and W. Wenner, U.S. Pat. 3,058,987, Oct. 6, 1962; Chem. Abstr., **58**, 5644c (1963).

(24) R. I. Geran, N. H. Greenberg, M. M. MacDonald, A. M. Schumacher, and B. J. Abbott, *Cancer Chemother. Rep.* (Part 3), **3** (Sept. 1972).

ACKNOWLEDGMENTS

The authors thank the Medical Research Council of Canada for the award of an operating grant (MA-5538) to J. R. Dimmock and the University of Saskatchewan for the award of a Graduate Scholarship to K. Shyam. Appreciation is recorded to the National Cancer Institute, Bethesda, Md., who undertook the antineoplastic evaluation of most of the compounds reported in this investigation.

Tack Behavior of Coating Solutions II

S. K. CHOPRA and R. TAWASHI ˣ

Received November 17, 1982, *from the Faculty of Pharmacy, University of Montreal, Case Postale 6128, Succursale "A", Montreal, Quebec, H3C 3J7 Canada.* Accepted for publication March 9, 1983.

Abstract □ The tackiness of coating solutions containing high concentrations of polymers was determined using a parallel plate technique. Kinematics of the film-splitting process was also investigated using a high-speed movie camera. The results showed that the impulse required to split a liquid film of highly concentrated polymer solution (semisolid), in contrast to a dilute solution is related not to viscosity, but to the internal structures of the system. Evidence has been found that the materials that are considered to be tacky in practice, display "delayed elastic effects" and require far larger impulses than nontacky materials.

Keyphrases □ Film-coating solutions—tablets, tack behavior, viscosity, concentrated polymer solutions □ Viscosity—film-coating solvents for tablets, tack behavior, concentrated polymer solutions □ Polymers—concentrated solutions, viscosity, tack behavior, film-coating of tablets

The technique of film-coating solid dosage forms has grown at an accelerating rate, employing a wide variety of materials and coating systems (1–3). One of the factors affecting the tablet-coating process is the tackiness of the coating formulations. The concentration of the film formers used in these coating formulations depends on the molecular weight, grade, and chemical structure of the polymers (4). Generally, the concentration of a polymer used in a film-coating formulation ranges from 2 to 10% (5). During the drying phase of the coating process, evaporation of the solvent occurs. Consequently, the concentration of the polymer increases, giving rise to increasing tackiness until the deposited film is essentially

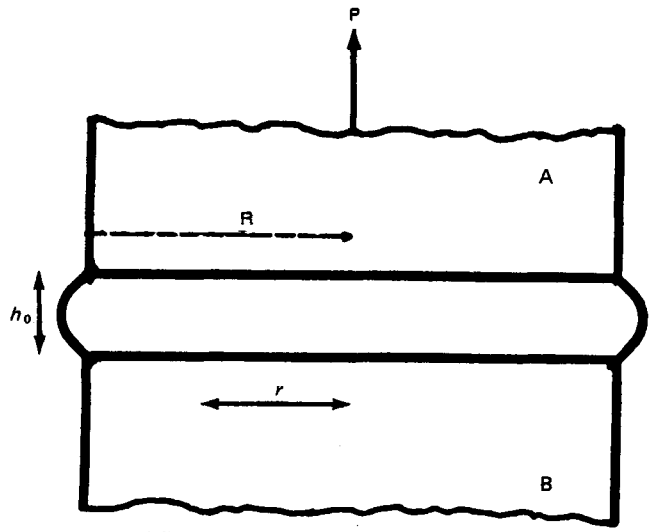

Figure 1—*Liquid flow between parallel plates.*

free of solvent (6). The tackiness of various coating solutions containing relatively low concentrations of polymers has been measured using a parallel-plate technique (7). The present study quantifies the tackiness of coating solutions containing high concentrations of polymers, *i.e.*, high-viscosity solutions.

BACKGROUND

In a previous communication (7), it was suggested that the relationship between tackiness and viscosity of coating solutions is nonlinear, and the following modified Stefan equation was proposed:

$$ft = \frac{3}{4} r^2 k' \eta^{0.67} \left[\frac{1}{h_1^2} - \frac{1}{h_2^2}\right] \qquad \text{(Eq. 1)}$$

where ft (tack) is the impulse per unit area required to separate two planes, initially in contact, through an intervening liquid; η is the viscosity (in poises) of the liquid; r is the radius (in centimeters) of the plates; h_1 and h_2 are the initial and final thickness (in centimeters) of the liquid film; and k' is the instrumental factor.

The above relationship was found to be satisfactory, provided that the rate of separation of plates joined with a liquid of given viscosity was below a certain limit. The upper limit of the speed of separation beyond which the experimental tack values obtained are lower than those predicted by Eq. 1 decreases with increase in the viscosity of a solution. An earlier study (8) on the tackiness of inks suggested that a rapid film separation does not occur by liquid flow, but is the result of a viscoelastic response of the liquid, which may react as a solid towards rapidly applied stress. This theory was later supported by another study performed on the kinematics of liquid film separation (9). Other studies (10, 11) acknowledged the existence of limits beyond which obedience to:

$$F = \frac{3\pi\eta r^4}{4t} \left[\frac{1}{h_1^2} - \frac{1}{h_2^2}\right] \qquad \text{(Eq. 2)}$$

by Stefan may not be expected, but the authors rejected the basic tenets of the viscoelastic theory in their explanation of film splitting at high rates of separation. These authors suggested that at high rates of separation, the flow conditions consistant with the above equation are upset by the onset of cavitation, which sets upper limits to the force of separation. On this basis the limiting force should be independent of the liquid and the initial distance between the plates. This is contrary to the results obtained experimentally. In the present study, an attempt is made to clarify the aforementioned discrepancies.

Consider two flat circular plates of radius R arranged parallel to each other

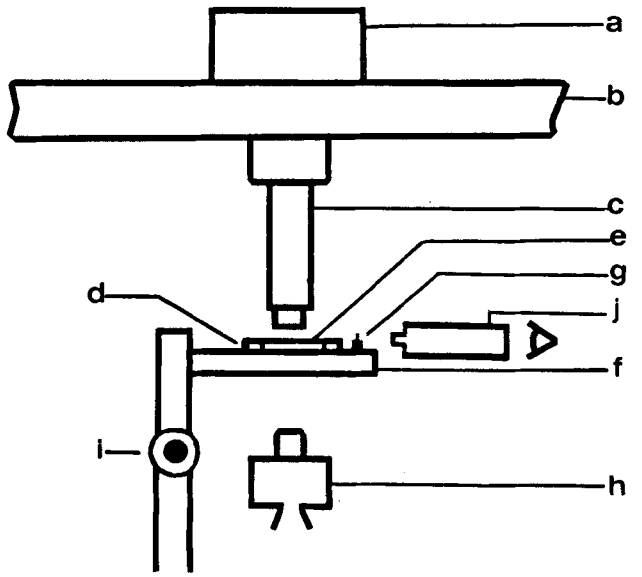

Figure 2—*Schematic diagram of tack measuring assembly in conjunction with a high-speed movie camera. Key: (a) load cell 500- or 5000-g capacity; (b) crosshead bar; (c) stainless steel probe r = 0.5642 cm; (d) stainless steel ring; (e) circular space; (f) glass plate; (g) pin; (h) high-speed movie camera; (i) knob for moving stage; (j) telemicroscope.*

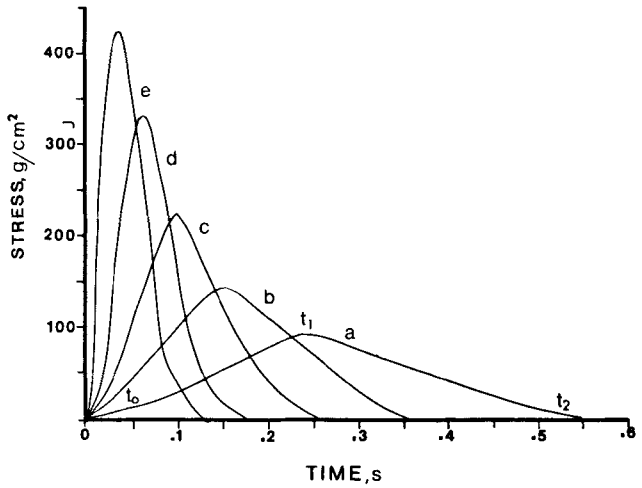

Figure 3—*Stress–time oscillograms at various rates of separation for 30% (w/w) aqueous solution of povidone. Key: (a) 8.33 × 10^{-3} cm/s; (b) 1.66 × 10^{-2} cm/s; (c) 3.33 × 10^{-2} cm/s; (d) 8.33 × 10^{-2} cm/s; (e) 1.66 × 10^{-1} cm/s.*

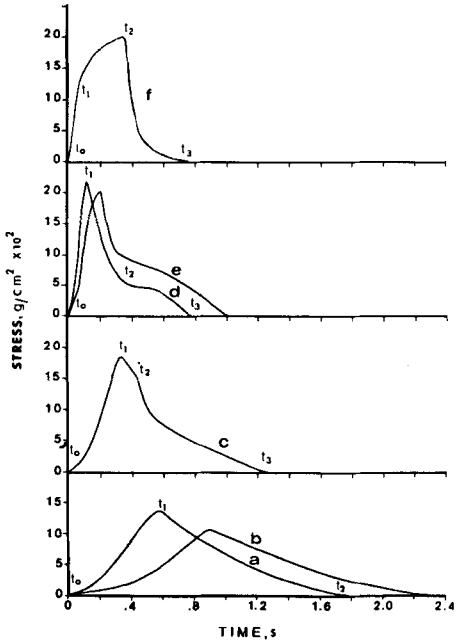

Figure 4—*Stress–time oscillograms at various rates of separation for 60% (w/w) aqueous solution of povidone. Key: (a) 3.33 × 10^{-3} cm/s; (b) 8.33 × 10^{-3} cm/s; (c) 1.66 × 10^{-2} cm/s; (d) 3.33 × 10^{-2} cm/s; (e) 8.33 × 10^{-2} cm/s; (f) 1.66 × 10^{-1} cm/s.*

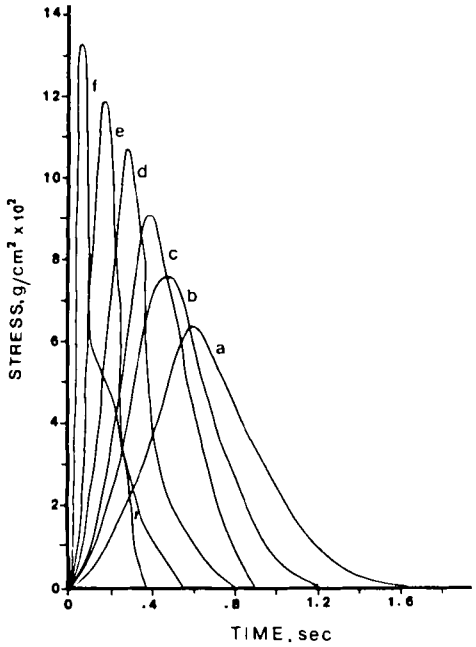

Figure 5—*Stress-time oscillograms at various rates of separation for lecithin. Key: (a) 3.33×10^{-3} cm/s; (b) 8.33×10^{-3} cm/s; (c) 1.66×10^{-2} cm/s; (d) 3.33×10^{-2} cm/s; (e) 8.33×10^{-2} cm/s; (f) 1.66×10^{-1} cm/s.*

and initially in contact through an interlayer of liquid of thickness h_0 (Fig. 1). When the plates are separated, the liquid from the periphery moves toward the center of the plates. This centripetal flow of the liquid is directly caused by the pressure difference between the peripheral and the central portion of the liquid layer (12).

When the distance h_0 between the plates increases by dh_0 in dt seconds, the volume of an imaginary cylinder of a radius r between the plates, increases by $\pi r^2 dh_0$. This volume increase is equal to the volume of liquid that must flow from the periphery into the above cylindrical space within the same time interval. The viscous force acting on the above volume of liquid of viscosity η is given by $\eta \cdot d^2u/dh^2 \cdot 2\pi \cdot r dr \cdot dh$. Here u is the linear viscosity of flow at the point (r,h). Therefore, the force F needed to separate the plates must be equal to the above viscous force. If the volume of liquid flowing at time dt into the cylindrical space $\pi r^2 dh_0$ is less than the latter, then the force F needed to separate the plates will be a fraction of the theoretical value.

With the increase in the concentration of a polymer in solution due to evaporation of the solvent during the coating process, a transition from low-viscosity solution to high-viscosity solution, followed by highly viscous solutions (semisolids) occurs, until a solid state is reached. In other words, the fluidity of the solution decreases with the increase in the concentration of the polymer. Therefore, it may be difficult for highly concentrated solutions of polymers to flow into the cylindrical space between the parallel plates according to the conditions described earlier. Furthermore, it is also likely that no flow occurs at all in the case of semisolids. Therefore, for highly concentrated solutions, the film separation process may be different from the one described above for the tack equation. Based on these considerations, experiments were designed to study simultaneously the kinematics and dynamics of the film separation process.

EXPERIMENTAL

Materials—Polymers used in this study were hydroxypropyl methylcellulose (5 cps)[1], hydroxypropyl cellulose[2], and povidone[3]. Solutions of polymers were prepared in distilled water. Lecithin[4], a Newtonian liquid, and white petrolatum[5], a semisolid gel, were also used.

Preparation of Solutions—The solutions of hydroxypropyl methylcellulose (5 cps) and hydroxypropyl cellulose were prepared by first dispersing the polymers in distilled water at 70°C and 50°C, respectively, and then cooling the dispersions with ice-cold water to 25°C to obtain clear solutions. The solutions of povidone were prepared by simply dissolving the polymer in water at 70°C. All solutions were allowed to stand at 25°C until free of air bubbles.

[1] Methocel "E" Premium (USP); The Dow Chemical Co., Midland, Mich.
[2] Klucel L F; Hercules, Wilmington, Del.
[3] Polyvinylpyrrolidone; Plasdone K 29-32; GAF Corp., Linden, N.J.
[4] Lecithin Technical; Anachemia Chemicals Ltd., Montréal, Canada.
[5] Ointment base No. 6; Penreco, Butler, Pa.

Table I—Tack Values of 30 and 60% (w/w) Aqueous Solutions of Povidone and Lecithin at Various Rates of Separation [a]

Rate of Separation, cm/s	ft, g/cm/s: Aqueous Solution of Povidone, 30% (w/w) (η = 0.93 poise)	Aqueous Solution of Povidone, 60% (w/w) (Pseudoplastic)	Lecithin (η = 62 poises)
3.33×10^{-3}	-	9.02×10^5	3.88×10^5
8.33×10^{-3}	2.30×10^4	9.45×10^5	3.87×10^5
1.66×10^{-2}	2.40×10^4	8.40×10^5	3.86×10^5
3.33×10^{-2}	2.45×10^4	7.65×10^5	3.75×10^5
8.33×10^{-2}	2.35×10^4	5.32×10^5	2.65×10^5
1.66×10^{-1}	2.42×10^4	6.28×10^5	1.87×10^5

[a] h_1 = 0.00108 cm.

Measurement of Viscosity—All measurements were made on a rotational cup-and-bob viscometer[6] in conjunction with a strip-chart recorder[7]. The temperature of solutions was held constant at 25°C. The cup-and-bob geometry was varied according to the viscosity of the sample.

Tack Measurement Assembly—Tack measurements were made using a tensile testing machine[8]. A schematic diagram of the tack measurement assembly has been described in our previous report (7).

Assembly for Kinematic Study—Figure 2 illustrates the setup of a 16-mm high-speed motion picture camera[9] in conjunction with the tack measuring assembly. The movie camera is capable of taking 4000 frames/s. A mechanical switching device simultaneously starts the movie camera and the upward movement of the crosshead bar (b) of the tensile tester.

Measurement of Film Thickness and Tack—The method for measuring the thickness of the liquid film has been described in our previous report (7). After adjustment of the thickness of the test liquid, the crosshead bar was allowed to move upward at a specified speed. The film separation events were recorded on a storage-type oscilloscope[10], where the separation force (F) was displayed as a function of time. All measurements were made at 25°C, and a minimum of six measurements were taken for every test solution at each separation rate. The experimental tack values were within a margin of error of ±6%.

RESULTS AND DISCUSSION

Tack Behavior of Solutions Containing High Concentrations of Polymers (High-Viscosity Liquids)—Rheograms of 30 and 60% (w/w) aqueous solutions of povidone revealed the former to be Newtonian, whereas the latter is pseudoplastic in nature. The stress-time oscillograms obtained at various rates of separation of these solutions are shown in Figs. 3 and 4, respectively, and show that as the time of separation decreases, the peak force of separation increases. This response by the above liquids is similar to the one reported for the solutions containing relatively low concentration of various polymers (7). The oscillograms for the 60% solution of povidone at rates of separation $\leq 8.33 \times 10^{-3}$ cm/s, are similar in shape to those for the 30% povidone solution at all rates of separation studied in this investigation. However, the oscillograms obtained for the 60% polymer solution vary in shape when the rates of separation are $>8.33 \times 10^{-3}$ cm/s. This change in shape of the oscillograms at higher rates of separation was also observed in the case of lecithin, a high-viscosity Newtonian liquid. In this case, the upper limit of the rate of separation beyond which the oscillograms begin to vary in shape is 1.66×10^{-2} cm/s (Fig. 5).

The tack values of the above solutions are given in Table I. The tack was calculated by dividing the area under the curves of the stress-time oscillograms by the surface area of the probe. Table I shows that for a 30% (w/w) aqueous solution of povidone, tack is independent of the rate of separation. This is in agreement with Eq. 1. However, the tackiness of the 60% polymer solution decreased with an increase in separation rates at $>8.33 \times 10^{-3}$ cm/s. This decrease in tack values cannot be attributed solely to the pseudoplastic nature of the above solution, since the tackiness of lecithin, a Newtonian liquid, also decreased at rates of separation $>1.66 \times 10^{-2}$ cm/s (Table I).

The above results suggest that there is an upper limit to the rate of separation beyond which the shapes of the oscillograms begin to vary, regardless

[6] Rotovisco; Brinkmann Instruments, Inc., Westbury, N.Y.
[7] Honeywell Electronik 194 Recorder; Honeywell Ltd., Montréal, Québec, Canada.
[8] Instron Tensile Tester Model 1122; Instron Canada, Burlington, Ontario, Canada.
[9] Hycam, Model #K20S4E; Kifer Industrial Park, Santa Clara, Calif.
[10] Model 5113 with 5B12N time base and two 5A26 dual differential amplifiers; Tektronix Inc., Beaverton, Ore.

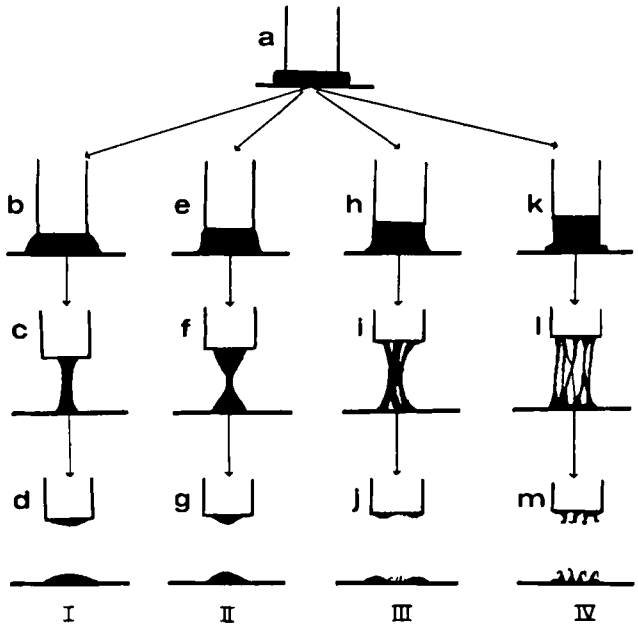

Figure 6—*Types of liquid flow patterns during film separation.*

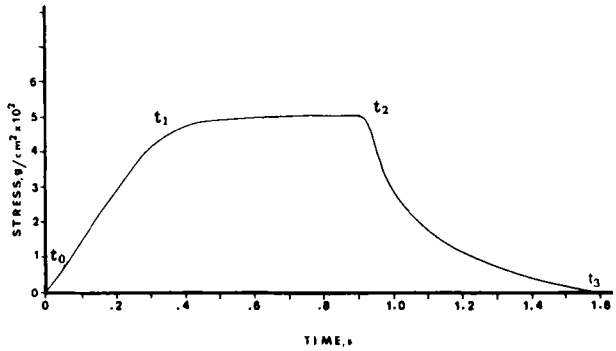

Figure 7—*Stress-time oscillogram at rate of separation of 8.33 × 10^{-2} cm for a 70% (w/w) aqueous solution of povidone;* h_1 = *0.00216 cm.*

of the flow behavior of the liquid. However, there is one noticeable difference between the shape of the oscillogram of lecithin and that of the 60% povidone solution obtained at a rate of separation of 1.66 × 10^{-1} cm/s. The slope of the ascending portion of the oscillogram (Fig. 5f) of lecithin is constant, whereas that for povidone solution (Fig. 4f) decreases gradually. The reason for this difference can be explained by simultaneously studying the kinematics and dynamics of the film-splitting process.

Kinematics of Film Splitting—The high-speed motion picture of the film separation process revealed four main patterns of liquid film splitting. The schematic diagrams of the film-splitting patterns as observed by projecting the high-speed movie are illustrated in Fig. 6.

Type I—Figure 6a–d represents the various stages of type I film-splitting pattern. The shapes of the oscillograms obtained for this pattern of film splitting are similar to those presented in Fig. 3. The first portion, *i.e.*, from t_0 to t_1 of the oscillogram (Fig. 3a), displays an increase in force which reaches a maximum. This is due to upward movement of the probe, which produces an increasing tension in the liquid until it begins to flow toward the center of the probe in order to relieve its strain (see Fig. 6b). The force required to maintain the centripetal flow is represented by the portion t_1 to t_2 of the oscillogram (Fig. 3a). This portion shows a gradual decrease in force from peak to zero. At t_2, the diameter of the base of the liquid column as seen from the bottom of the glass plate is at its minimum. Any further increase in the gap between the probe and the plate does not lead to further centripetal movement of the liquid, but rather to a necking-down of the column which eventually splits (see Fig. 6d). In cases such as above, the experimental *ft* is equal to that calculated using Eq. 1. Therefore, this pattern of liquid film splitting is in accordance with the theoretical consideration.

Type II—The various stages followed by the type II pattern of liquid film splitting are shown sequentially in Fig. 6e–g. The corresponding oscillogram is presented in Fig. 4c. The increase in force exhibited by the oscillogram from t_0 to t_1 is due to the increase in strain in the liquid before it begins to flow. The initial velocity of centripetal flow of the liquid is slower than the corresponding vertical movement of the probe. During this period a rapid decrease in force occurs. This is represented by the oscillogram (Fig. 4c) from t_1 to t_2. From t_2 to t_3, the velocity of the centripetal flow of the liquid increases, but does not keep pace with the rate of increase in the gap between the probe and the plate. During this time interval, the force gradually decreases to zero. At t_3, the diameter of the base of the liquid column is larger than that shown in Fig. 6f. The final separation takes place by necking-down of the hourglass column (Fig. 6g). The above observations clearly show that the centripetal flow of the liquid is not achieved within the time of creation of the cylindrical space between the probe and the plate. This means that the conditions described for the tack equation are not met. Therefore, in this type of film separation pattern, the value of experimental *ft* is less than that predicted by Eq. 1.

Type III—The oscillogram (Fig. 4d) corresponds to the film separation sequence shown in Figs. 6h–j. As soon as the tension in the liquid reaches its maximum, *i.e.*, at t_1 in Fig. 4d, the liquid begins to move centripetally but in irregular fashion. This type of movement leads to "channeling" of the liquid and produces a rapid decrease in force as shown by the portion t_1 to t_2 of the oscillogram. The liquid in channel form continues to move toward the a[x]is of the plate. This results in a gradually decreasing force as depicted by t[h]e portion t_2 to t_3 of the trace. The column arising out of the channeled liqu[id] is not cylindrical (Fig. 6i). The channel formation of the liquid (Fig. 6j) c[an] be seen even after film splitting. As in type II, the value of the experimen[tal] *ft* is lower than the predicted value.

Type IV—The oscillogram (Fig. 4f) corresponds to the film-splitting sequence shown in Figs. 6k–m. When the strain in the liquid is increased, a rapid linear increase in force from t_0 to t_1 is recorded. From t_1 to t_2, an increase in force continues but with decreasing slope. Since no centripetal flow occurs from t_0 to t_2, the decreasing slope of the increasing stress from t_1 to t_2 could be attributed to the orientation of polymer molecules toward the direction of flow, thereby reducing the internal resistance of the material until the flow begins (12). With the further increase in the gap between the probe and the plate, the liquid moves toward several points instead of moving toward the center of the plate. This eventually leads to the formation of several filaments (Fig. 6m). During this time, the separation force decreases, first rapidly and then gradually until it reaches zero, at t_3.

The increase in force with decreasing slope as shown by the portion t_1 to t_2 of the oscillogram for povidone (Fig. 4f) was also observed in the case of 30% (w/w) aqueous solution of hydroxypropyl methylcellulose (5 cps) and 30% (w/w) aqueous solution of hydroxypropyl cellulose. However, in the case of lecithin, the ascending portion of the oscillogram (Fig. 5) showed a linear increase in force at all rates of separation.

The results of this simultaneous kinematic and dynamic study of the film separation process suggest that the separation force reaches a maximum before the centripetal flow of the liquid takes place. The rate of increase in force during this time, remains constant if the resistance is purely viscous. A decrease in the rate of increase in force occurs in the case of highly concentrated polymer solutions and is probably due to the rearrangement of the internal structure of the system. The portion of the oscillogram representing maximum to zero separation force is dependent on the centripetal flow of the liquid during film separation. The shape of this region of the oscillogram changes with the change in pattern of the centripetal flow, which in turn is dependent on the viscosity of the liquid and the rate of film separation.

Tack Behavior of Highly Concentrated Polymer Solutions (Semisolids)—The stress-time oscillogram for a 70% (w/w) aqueous solution of povidone obtained at a rate of separation of 8.33 × 10^{-2} cm/s is shown in Fig. 7. The film separation process indicated that no centripetal movement of the liquid occurs and that film splitting proceeds by simple stretching and thinning-down of the filaments. Therefore, the film-separation process is different from that described for low- and high-viscosity solutions.

The stress-time oscillogram obtained is to a certain extent close to the stress-strain curve exhibited by the ductile response of plastics at high rates of separation (13). It can be divided into three regions. The first region represented by the portion t_0 to t_1 of the oscillogram (Fig. 7) is predominently due to the elastic forces of the liquid. In this region, the force first rises proportionally to the elongation and then rises less rapidly until it reaches "yield point" at t_1. In the second region following the "yield point," the specimen offers a pull resistance which is constant over a long period of time: t_1–t_2. Since no centripetal flow takes place during this time, the force is mainly due to the resistance to elongation of the filament beyond the elastic limit. This second region of the curve has been suggested to be due to the "delayed elastic deformation" effects (14). In the third region, t_2–t_3, "necking" and eventually splitting of the filaments occur. In Fig. 7, the *ft*, 9.80 × 10^4 g/cm/s for thinning and final rupture of the filament is only 20% of the total 4.81 × 10^5 g/cm/s required for the separation of the film. The bulk of the *ft*, 3.83 × 10^5 g/cm/s is devoted to the process of film elongation.

Tack experiments performed with petrolatum, a highly viscous semisolid did not show the region of "delayed elastic effects." This resulted in a rather short duration for filament elongation; hence the ft was relatively small.

The above observations suggest that the response of the concentrated polymer solutions (semisolids) to applied pull stress is a combination of viscous and elastic forces. The "delayed elastic effects" observed are the result of configurational elasticity, which is a process associated with orientation, alignment, and elongation by the uncurling of large chain molecules. Therefore, the ft required for the elongation of the filament will not only depend on the viscosity of the liquid, but also on the internal structure of the system.

Earlier investigators (10–12) suggested that tackiness is related to the geometry of the system and the rheological characteristics of the liquid. Therefore, according to this definition, lecithin, petrolatum, and even water added with high concentration of finely divided solids will be considered tacky, since these liquids or dispersions do offer resistance to flow. In actual practice, the above materials, unlike povidone solution, are not known to be tacky even though impulse for liquid film separation is required in both cases. Based on these observations, it can be concluded that a tacky material is one that displays "delayed elastic effects," and because of these effects it requires a long period of time for filament elongation. This provides a rather large impulse for a given force of separation.

Tack Effects in Tablet Coating—Coating solutions, when applied to the tablets during the coating process, are dilute solutions of polymers of low-viscosity grade. Separation of tablets stuck together by a freshly applied coating solution will occur by viscous flow. Therefore, the ft required will be equal for solutions of similar viscosity. As the solvent evaporates during the drying phase of the coating process, the solution will reach a semisolid state. At this point, resistance to filament elongation will depend on the molecular structure of the polymer.

Tablet coating solutions usually contain opacifier, plasticizers, and colorants to modify the physical characteristics and improve the film-forming properties of the polymers. The effect of these additives on the tack behavior of coating solutions is under investigation.

REFERENCES

(1) S. C. Porter, *Pharm. Tech.*, **4**(3), 67 (1980).

(2) H. A. Lieberman and L. Lachman, "Pharmaceutical Dosage Forms: Tablets," Vol. 3, Dekkar, New York, N.Y., 1982, pp. 73–117.

(3) J. Cooper and J. E. Rees, *J. Pharm. Sci.*, **61**, 1511 (1972).

(4) J. R. Cloche, *Labo-Pharma*, **157**, 41 (1967).

(5) "Cellulose Ethers in Aqueous System for Tablet Coating," Dow Chemical Co., Midland, Mich., 1977, p. 4.

(6) N. O. Lindberg and E. Jonsson, *Acta Pharm. Suecica*, **9**, 589 (1972).

(7) S. K. Chopra and R. Tawashi, *J. Pharm. Sci.*, **71**, 907 (1982).

(8) A. Voet and C. F. Geffken, *Ind. Eng. Chem.*, **43**, 1614 (1951).

(9) R. A. Erb and R. S. Hanson, *Trans. Soc. Rheal.*, **1**, 3 (1957).

(10) W. H. Bank and C. C. Mill, *J. Colloid Sci.*, **8**, 137 (1953).

(11) H. Strasburger, *J. Colloid Sci.*, **13**, 218 (1958).

(12) J. J. Bikerman, *J. Colloid Sci.*, **2**, 163 (1947).

(13) S. S. Voyutskii, "Autohesion and Adhesion of High Polymers," Interscience, New York, N.Y., 1963, pp. 235–248.

(14) A. D. Jenkins, "Polymer Science," American Elsevier, New York, N.Y., 1972, pp. 775–800.

ACKNOWLEDGMENTS

This work was supported by the Medical Research Council of Canada.

Phase Diagram and Aqueous Solubility of the Lidocaine–Prilocaine Binary System

A. BRODIN *x, A. NYQVIST-MAYER *, T. WADSTEN ‡, B. FORSLUND ‡, and F. BROBERG *

Received December 28, 1982, from the **Astra Läkemedel AB, Research and Development Laboratories, Pharmaceutics, S-151 85 Södertalje* and the ‡*Arrhenius Laboratory, University of Stockholm, Fack, S-106 91 Stockholm, Sweden.* Accepted for publication February 17, 1983.

Abstract □ The phase behavior of the lidocaine–prilocaine binary system has been studied by X-ray diffraction, differential thermal analysis, hot-stage microscopy, and IR spectrometry. No intermediate compounds or solid solubilities have been detected. The eutectic composition is close to 1:1, and the eutectic temperature is 18 ± 1°C. Aqueous solubility studies show that the lidocaine heat of solubility from the eutectic mixture is different from that of the pure drug, whereas it is the same for prilocaine. Investigations of various lidocaine–prilocaine ratios indicate that the two local anesthetics decrease the solubility of each other. The total solubility, however, is affected only to a minor extent.

Keyphrases □ Lidocaine—binary system with prilocaine, phase diagram and aqueous solubility □ Prilocaine—binary system with lidocaine, phase diagram and aqueous solubility □ Solubility—phase diagram of the lidocaine–prilocaine binary system in water □ Phase diagram—lidocaine–prilocaine binary system, aqueous solubility

Solid–solid interactions are of great interest in the development of pharmaceutical preparations. Dissolution rates, and thus bioavailability, of poorly soluble drugs can be enhanced by their fusion with water-soluble carriers such as urea or polyethylene glycol, which form solid solutions with drugs (1, 2). Eutectic mixtures may even be used to prevent freeze–thaw coagulation of suspensions (3). In powder technology, on the other hand, a eutectic interaction between substances may be considered as an incompatibility, making it necessary to use some auxiliary substance to inhibit adhesion of the powders (4). The physical state in which the drugs are present in such fused mixtures is debatable. The dispersion of phenylbutazone in urea represents a "plug compound" (5). Such solid dispersions are known to age (6, 7).

Studies on eutectic combinations of two drugs are rare (8). Recently, lidocaine and prilocaine have been reported to form a eutectic mixture (9). Since this mixture is liquid at room temperature, it has been possible to formulate an effective local anesthetic preparation for topical application. The purpose of this investigation is to characterize the lidocaine–prilocaine system from a physical point of view and to study its aqueous solubility.

EXPERIMENTAL

Materials—Lidocaine[1] and prilocaine[1] were used as obtained. To prepare the eutectic mixture (EMLA), 49.6% lidocaine and 50.4% prilocaine by weight were mixed and heated gently until liquefaction occurred.

X-Ray Diffraction—An X-ray powder diffraction camera[2] with a 50-mm diameter and strictly monochromatized Cu$K\alpha_1$ radiation was used. A small amount of the powder was spread out on the glue side of ordinary tape. The tape was attached to a thin metal plate, 30 mm in diameter, with an 8-mm

[1] Astra Pharmaceutical Production AB, Sweden.

[2] Guinier-Hägg.

0022-3549/84/0400-0481$01.00/0